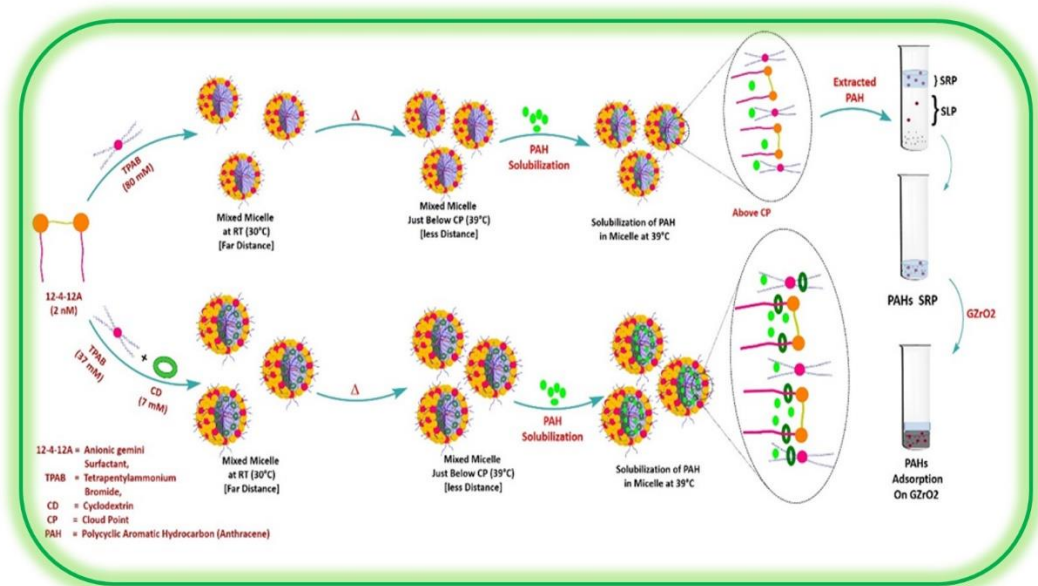


Chapter 4

Solution Behavior of Anionic Gemini Modified Surface Active Ionic Liquid: Interaction; Clouding and Solubilization



Published in J. Mol. Liq. 2018, 272, 413-422.

4.1. Introduction

Ionic liquids are novel solvents with great potential across many interfaces of scientific research due to this reason, they harvest great interest which is clear from the number of publication appeared in the literature [1, 2]. Ionic liquids combining with quaternary ammonium cation have been shown more efficient than the first generation of ionic liquids. In the bulk aqueous phase, the ionic liquids with long hydrocarbon tail show self-organized micelle type structures ranging from an ion pair to aggregates [3-5]. Such type of ionic liquids can be called surface active ionic liquids (SAIL) [6,7] whose degree of aggregation depends upon the alkyl chain and central atom (N or P)[8]. A few types of research focused on the ionic liquids halide counter-ions, especially for bromide (Br⁻) counter-ion [9-13]. Moreover, SAIL is liquids in a wide range of temperatures, high chemical, and thermal stability and are able to solvate solute from a large spectrum of polarities.

As mentioned in chapter 1, the aqueous surfactant solution display single phase below CP and under goes liq-liq phase separation above it (*clouding phenomenon*). This phenomenon rarely observed with ionic surfactant solutions. This may be due to the electrostatic repulsive interaction between the head groups (or charged micelles) that can work against the occurrence of CP phenomenon. However, CP phenomenon, with conventional anionic surfactants (SDS, SDBS or sodium oleate), was observed in the presence of both symmetrical and unsymmetrical quaternary salts such as tetra-n-butyl ammonium bromide (TBAB), tetra-n-butyl phosphonium bromide (TBPB) and n-propyl triphenyl phosphonium bromide [13-17].

As mentioned above, both ionic surfactant and SAIL are not showing clouding phenomenon alone at ambient conditions. Literature data suggest that clouding and

phase separation could be possible by judicious mixing of an anionic surfactant and SAIL. However, CP data with gemini surfactants are not much to optimize the system. Gemini surfactant, having spacer group, may provide an additional attractive force which may make CP behavior to occur at least in principle. Therefore, it is of genuine interest to study the solution behavior of a SAIL with or without a gemini surfactant. It has been reported that the balance of interaction affects the efficiency of migration of biomolecules in mixed systems showing liq-liq phase separation [18, 19]. However, the mixing of surface active ionic liquids with gemini surfactants has not been studied many times [20, 21].

Keeping above view in mind, micellization and CP behaviors of a SAIL (tetra-n-pentyl ammonium bromide, TPeAB) have been studied in the presence of an anionic gemini surfactant, 12-4-12A in aqueous solution. *cmc* and NMR data suggest about the degree of non-ideality of the interaction in the mixed micelle using Rubingh's Non-ideal solution theory [22]. Various quaternary bromides were added to the 12-4-12A solution, only TPeAB have shown clouding phenomenon at certain specific compositions. This composition was further optimized with the help of biomolecules (amino acids and cyclodextrin). Recently, cyclodextrin solutions have also been used for the extraction of various PAHs from the contaminated soil [23]. DLS, POM, and TEM data were acquired to gain information related to the morphology of the mixed system at ambient temperature and near the cloud point. A few such optimized systems were used for solubilization/ co-solubilization studies with various PAHs. These solubilized systems were used for cloud point extraction of above PAH in the surfactant-rich phase (SRP). Gr@ZrO₂-NC has shown good adsorption capacity for PAH. The solubilized/adsorptive removal of nearly water insoluble PAHs may find application for recharging of aquatic/ solid soil matrices.

4.2. Results and Discussion

4.2.1. Micellization of Single TPeAB and 12-4-12A

Tensiometry (Figures 1a and 2a) and conductometry (Figures 1b and 2b) measurements result in almost similar *cmc*s for TPeAB and 12-4-12A, respectively (Table 1) which indicate the validity of the measurement.

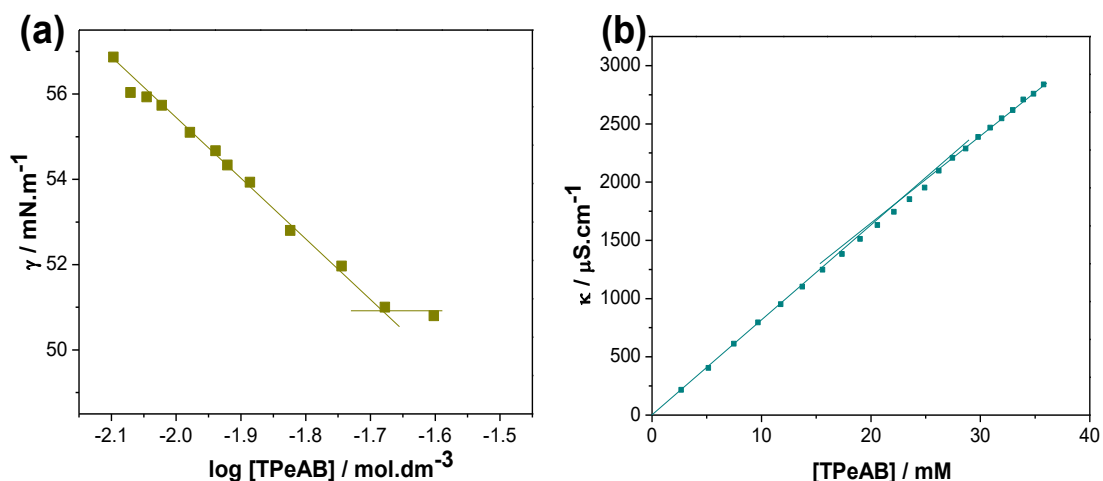


Figure 1. (a) Plots of surface tension (γ) vs log C (logarithm of concentration) and (b) plot of specific conductance (κ) vs concentration of surface active ionic liquid (TPeAB) in aqueous solution at 30°C.

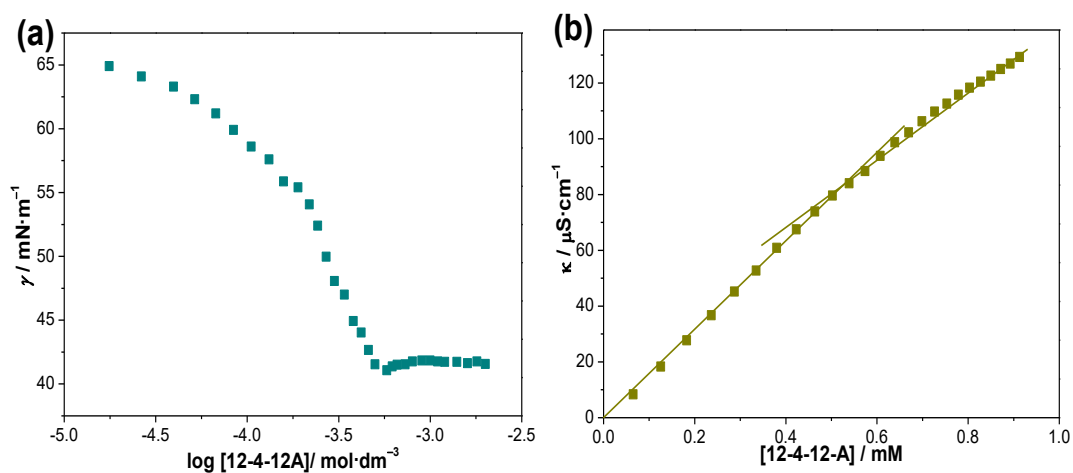


Figure 2. (a) Plot of surface tension (γ) vs log C (logarithm of concentration) and (b) plot of specific conductance (κ) vs concentration of anionic gemini surfactant (12-4-12A) in aqueous solution at 30°C

TPeAB has much higher *cmc* than 12-4-12A (Table 1). This may be due to the presence of lower alkyl chain length in TPeAB. The absence of a minimum in the plot of surface tension (γ) vs log C (Figure 2a) ensures the purity of the 12-4-12A. In the solution, TPeAB furnishes TPeA⁺ (positively charged surface-active species) and Br⁻. This can interact with anionic micelle (of 12-4-12A) and may produce synergistic interactions (electrostatic interaction). In the next section (4.2.2), such interactions are studied by *cmc* measurements (conductometrically) at various mole fractions of TPeAB and 12-4-12A.

Table 1. Critical micelle concentration (*cmc*) of surface active ionic liquid (TPeAB) and anionic gemini surfactant (12-4-12A) at 30 °C

Surfactants	<i>cmc</i> (mM)	
	Conductometry	Tensiometry
12-4-12A	0.55	0.50
TPeAB	20.5	20.6

4.2.2. Mixed Micellization of TPeAB with 12-4-12A

cmc measurements (Figure 3) have also been performed in the mixed aqueous system (TPeAB + 12-4-12A) at various mole fractions and data are compiled in Table 2. *cmc* variation with a mole fraction of added TPeAB, to 12-4-12A, has been shown in Figure 4. A pseudo phase separation model has been applied to evaluate how the *cmcs* of binary mixtures (TPeAB + 12-4-12A) deviate from the ideal mixing [22]. The *cmc* values of the mixture (cmc_{exp}) are found lower than the individual components of the mixture (12-4-12A(cmc_1) or TPeAB (cmc_2)).

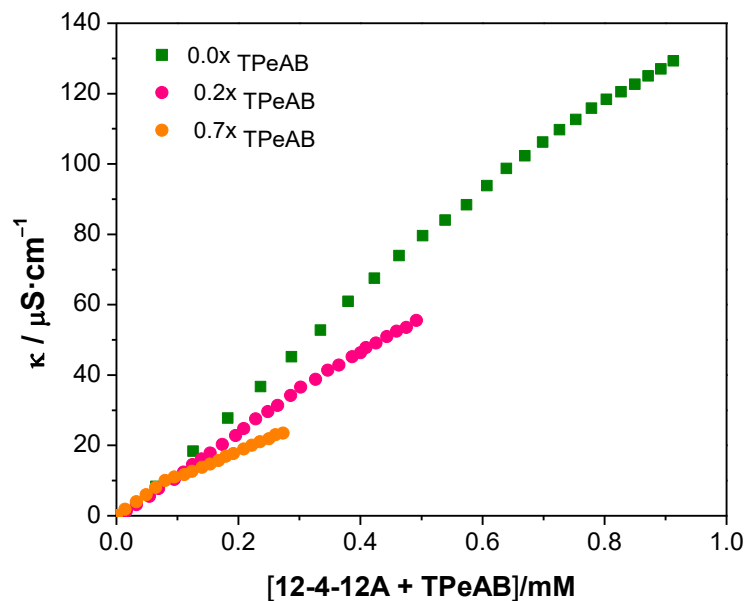


Figure 3. The plot of specific conductance (κ) vs concentration of pure 12-4-12A and representative 12-4-12A + TPeAB mixed systems at two different mole fractions of surface active ionic liquid (x_{TPeAB}) in aqueous solution at 30°C.

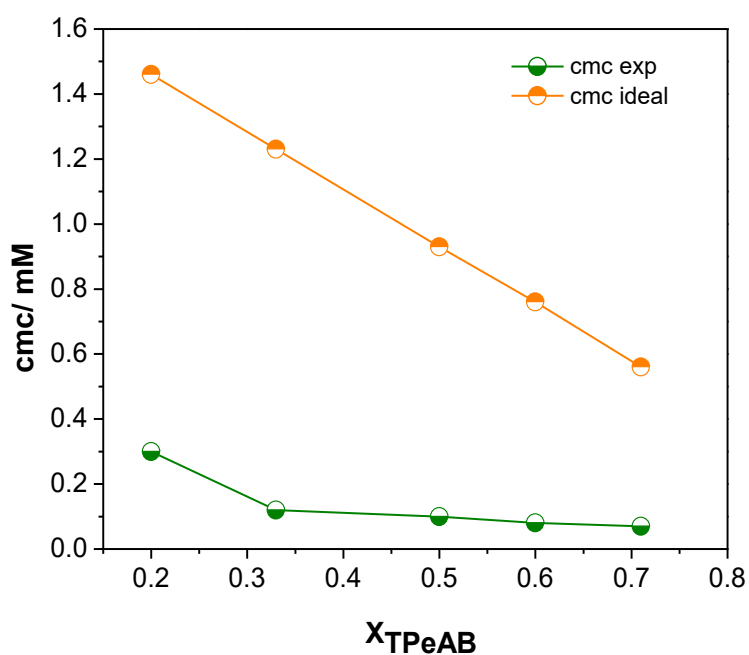


Figure 4. Critical micelle concentration (*cmc*, by conductometrically) variation of mixed system (12-4-12A + TPeAB) with mole fraction of TPeAB (x_{TPeAB}) in aqueous solution at 30 °C. The plot represents experimental and ideal values (calculated from Clint model).

For a mixture of oppositely charged surfactant and surface active ionic liquid (TPeAB), a relation (Equation 1) exists for ideal mixing [24].

$$\frac{1}{cmc_i} = \frac{x_1}{cmc_1} + \frac{x_2}{cmc_2} \quad (1)$$

where, x_1 and x_2 are mole fractions of 12-4-12A and TPeAB, respectively. The cmc for ideal mixing (cmc_{ideal}) of oppositely charged components can be determined using equation 1. The negative variation of cmc_{exp} from cmc_{ideal} (Figure 4) indicates synergistic interaction in various mixtures (Table 2). Following expression (Equation 2) has been proposed based on regular solution theory [25].

$$\frac{[(X_1^m)^2 \ln(cmc_{exp} x_1 / cmc_1 X_1^m)]}{(1-X_1^m)^2 [cmc_{exp} (1-x_1) / cmc_2 (1-X_1^m)]} = 1 \quad (2)$$

X_1^m denotes the mole fraction of 12-4-12A in the mixed micelle. The Ideal micelle mole fraction of 12-4-12A (X_1^i) can be calculated using Motomura's approximation [26].

$$X_1^i = \frac{x_1 cmc_2}{x_1 cmc_2 + (1-x_1) cmc_1} \quad (3)$$

Mostly, the interaction parameter (β^m) has been used to understand the nature and strength of the interactions between different amphiphilic molecules (constituting the mixture) and can be obtained by applying following expression (Equation 4) [27],

$$\beta^m = [\ln(cmc_{exp} p_1 / cmc_1 X_1^m)] / (1 - X_1^m)^2 \quad (4)$$

As cmc_{exp} has been found lower than the cmc_i , β^m values are expected to be negative in each case (synergistic effect). This indeed was observed (Table 2). The behavior is the result of the packing of each component in the mixed micelle (and the resultant cmc_{exp}). The data related to cmc_{exp} , cmc_{ideal} , cmc_1 , cmc_2 , X_1^m , X_1^i and β^m are

tabulated in Table 2. Details of various NMR peaks and respective protons for TPeAB and 12-4-12A are given Figure 5.

Table 2. Micellization parameters (critical micelle concentration, cmc , by conductometrically) and interaction parameters (by using Rubingh's method) of mixed system (12-4-12A and TPeAB) at different mole fraction (x) in aqueous solution at 30°C.

x_{TPeAB}	$cmc_{exp}(mM)$	$cmc_{ideal}(mM)$	X_1^m	X_{ideal}	β^m
0.0	0.55	-	-	-	-
0.2	0.30	1.46	0.743	0.993	-8.10
0.33	0.12	1.23	0.651	0.987	-12.39
0.5	0.10	0.93	0.619	0.974	-13.19
0.6	0.08	0.76	0.598	0.961	-14.41
0.71	0.07	0.56	0.578	0.939	-15.46
1.0	20.5	-	-	-	-

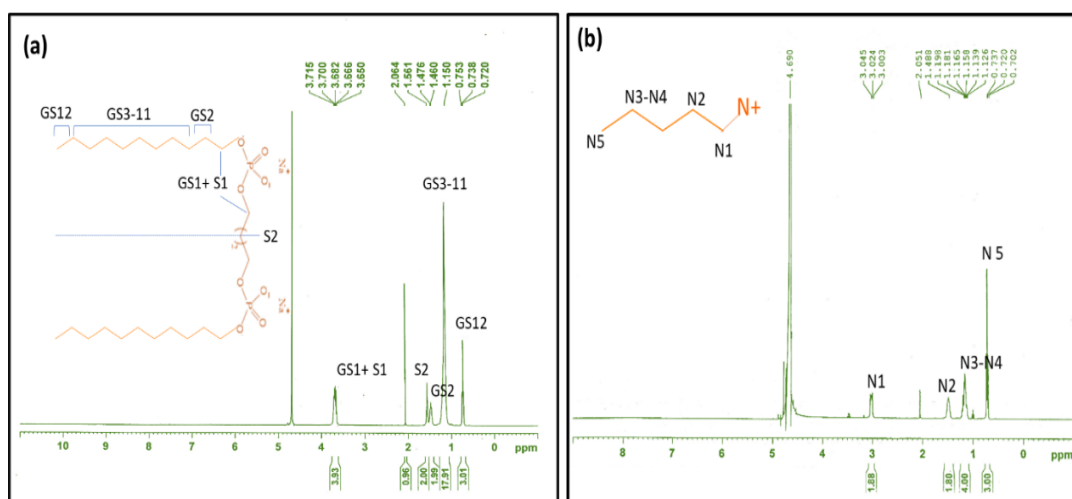


Figure 5. (a) 1H NMR spectrum of anionic gemini surfactant 12-4-12A, (b) surface-active ionic liquid TPeAB at 30°C.

2D NOESY spectra of TPeAB+ 12-4-12A solution have been shown in Figure 6. Intermolecular interaction is clearly reflected from the cross peaks shown in 2D NOESY spectra. Cross peaks between N1-N3/N4, N1-N2, and GS1-N3/N4 protons show space interactions which indicate intercalation of pentyl chain of TPeA⁺ between gemini monomers of the micelle (mixed micelle). Probably this interaction of chains (pentyl and dodecyl of SAIL and 12-4-12A, respectively) is responsible for negative β_m value (synergistic effect) as has been discussed above. The possible effect of the above interactions on the solution behavior has been discussed in the next section (4.3).

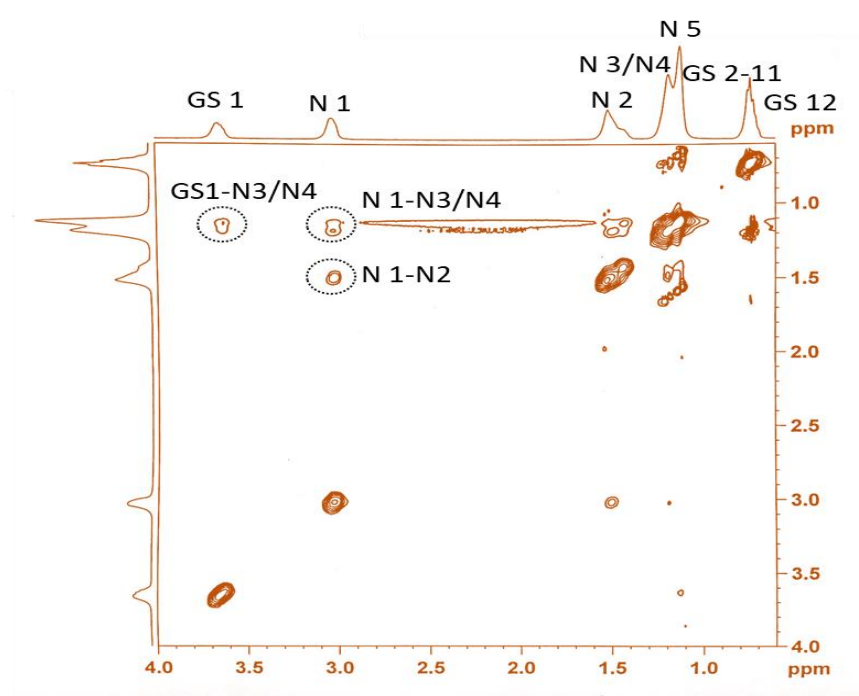


Figure 6. 2D NOESY ¹H NMR spectra of the mixed system (2 mM 12-4-12 A + 2 mM TPeAB) in D₂O.

4.3. Clouding Behaviour

4.3.1. Clouding Phenomenon in Aqueous TPeAB with 12-4-12A

Many SAILs (quaternary salts) have been tried in combination with 12-4-12A to observe the appearance of the clouding phenomenon at elevated temperature. However, the phenomenon has been observed only with TPeAB. CP variation with

[TPeAB] has been shown in Figure 6. CP data for TPeAB + SDS (well-known anionic surfactant showing CP with TPeAB) aqueous system are also included in Figure 7 for comparison purposes. A perusal of CP data shows that more amount of TPeAB is required to observe CP with 12-4-12A than SDS (for equal [surfactant], 10 mM). This may be due to the fact that 12-4-12A has two anionic $-\text{PO}^{4-}$ head groups which require more SAIL (TPeAB) to neutralize the head group(s) charge. The appearance of clouding in such mixed systems has been explained in terms of van der Waals, electrostatic and hydrophobic interactions together with heating induced dehydration of the micellar surface headgroups [28]. The TPeA⁺ contains four *n*-pentyl chains, in addition to a positive charge on the central N- atom, therefore, the cation can interact with the negatively charged micellar surface (electrostatically) as well as interior part of the anionic micelle (hydrophobically). Due to the above interactions, micelles would be of much lower charge (pseudo-nonionic) and larger size (with close interactions among them through *n*-pentyl chains). Above factors seem responsible for dehydrated micelle and the observed clouding behavior. The mechanism is well supported by earlier studies [29-32].

DLS and zeta-potential data (Figure 8 and Table 3) support the above proposition of increased micellar size and lowering of micellar charge as the system moves towards CP on heating. Two morphologies have been shown by DLS results. However, higher aggregate sizes are chosen to compile Table 3. This is due to the fact that bigger aggregates distinctly contribute to clouding [28].

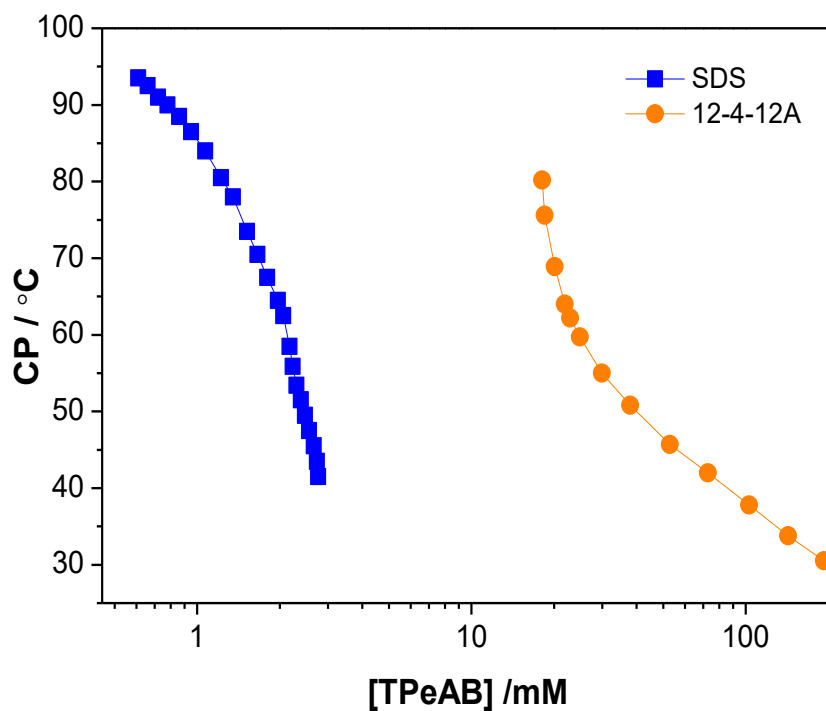


Figure 7. Cloud Point (CP) of anionic conventional (sodium dodecyl sulfate, SDS) and gemini surfactant (12-4-12A) as a function of the concentration of TPeAB.

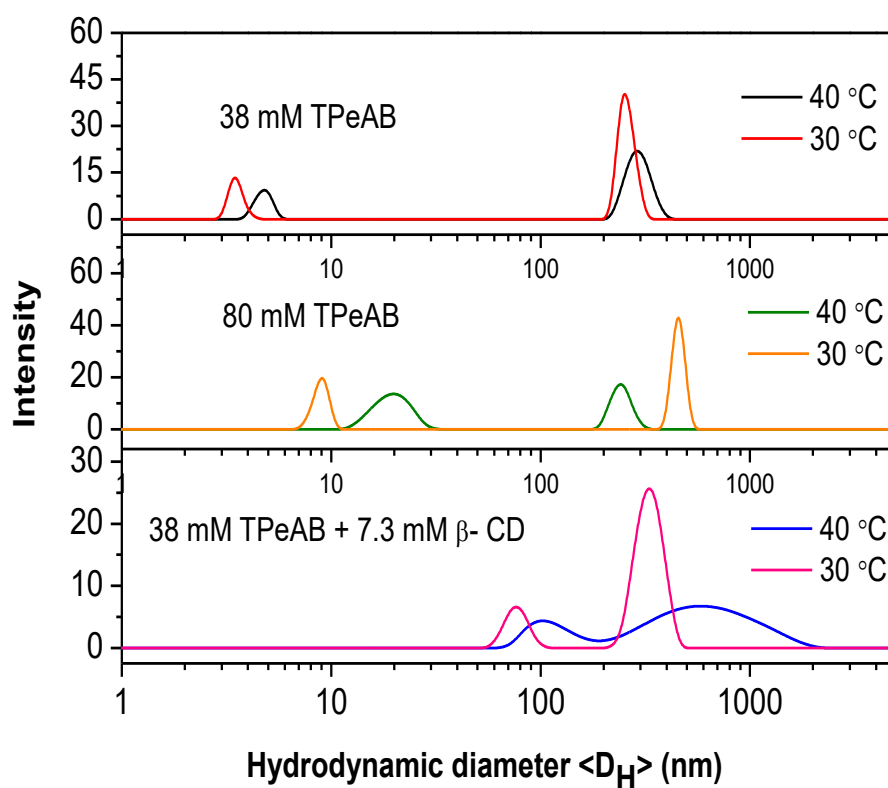


Figure 8. DLS data for 2mM 12-4-12A + 38 mM (or 80mM) TPeAB with (a) and without β -CD (b, c)

Figure 9 shows that there exists a well-defined value of [TPeAB] for a particular [12-4-12A]. The exact relationship between [TPeAB] and [12-4-12A] can be obtained by fitting straight-line plots using linear regression (Table 4). Regression data can be used to determine concentrations of gemini surfactant and SAIL to get CP at the desired temperature.

Table 3. Average hydrodynamic data ($\langle D_H \rangle$) and Zeta (ζ)- potential values for various mixed System at two different temperatures (T).

System	$\langle D_H \rangle$		ζ - potential	
	30 °C	40 °C	30 °C	40 °C
2 mM 12-4-12A + 80 mM TPeAB	9.1, 461	19.8, 252	-2.6	-1.2
2 mM 12-4-12A + 38 mM TPeAB	3.7, 256	4.8, 295	-13.4	-9.2
2 mM 12-4-12A + 38 mM TPeAB + 7.3 mM β - CD	75.2, 328	101.5, 602	-14.3	-12.3

To see the influence of temperature on micellar structures, POM micrographs (Figure 10) were acquired at room temperature, just below and at the CP. This study shows that the size of the aggregates increases as the system approaches the CP. This observation has been in consonance with the DLS results discussed above. The increase in aggregate size may be due to dehydration and charge depletion of the micellar surface region together with *n*-pentyl chain mediated linking of aggregates [28, 30, 33, 34].

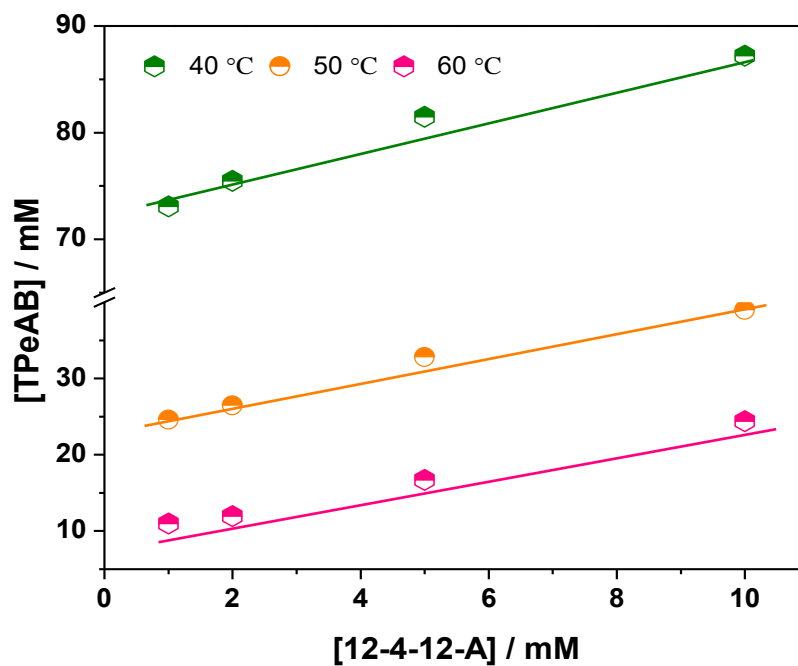


Figure 9. The interplay between [12-4-12A] and [TPeAB] to obtain CP at 40, 50 or 60°C.

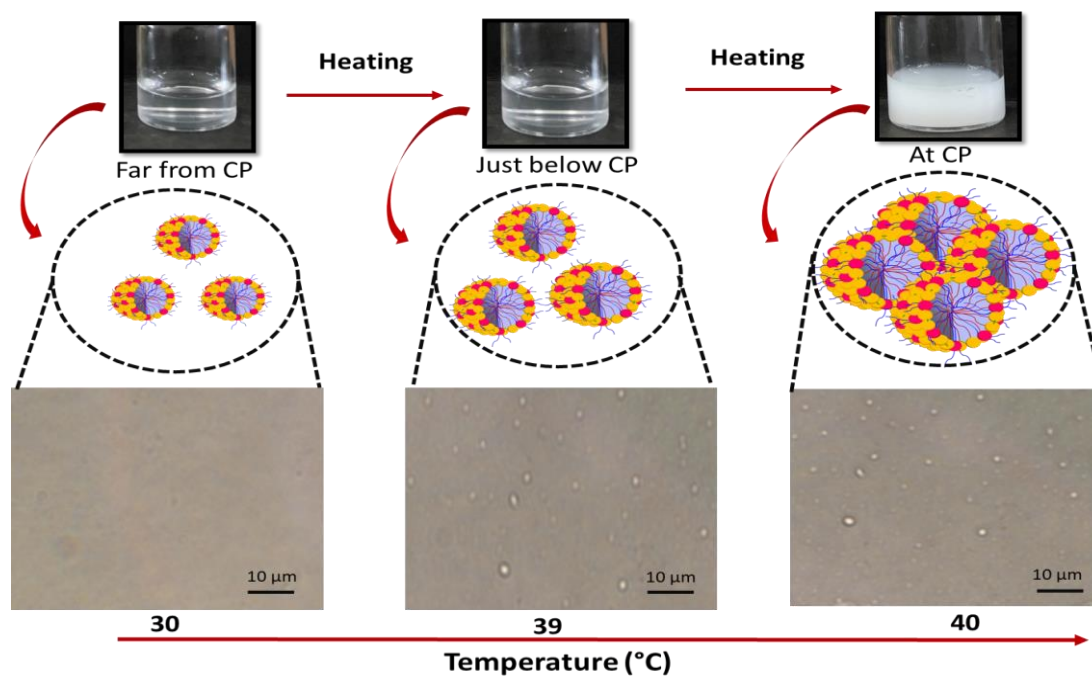


Figure 10. Polarizing optical micrographs of 2 mM 12-4-12A + 80 mM TPeAB aqueous system at different temperatures.

Table 4. Linear Regression data for conventional (SDS) and gemini (12-4-12A) surfactant for the interplay of [surfactant] – [TPeAB] to get CP at different temperature (40-70 °C)

CP (°C)	SDS ^a			12-4-12 A ^b		
	S	I	R	S	I	R
40	-	-	-	1.55	72.35	0.984
50	0.279	2.877	0.997	1.60	23.48	0.986
60	-	-	-	1.51	9.20	0.998
70	0.271	1.448	0.998	-	-	-

4.3.2. Effect of Biocompatible Additive on Clouding Behavior

Figure 11 shows the variation of CP with bio-additives (β -CD and glycine). 12-4-12A is expected to form an inclusion complex with CD's, affecting the aggregation process of the gemini itself [35]. Further, β -CD has been reported to form 1:1 complex with anionic surfactants [36]. The CP behavior of TPeAB +12-4-12A shows similar CP decrease with both β -CD and glycine. However, CP decreasing power of β -CD has been found more than glycine. β -CD contains various hydroxyl groups (and typical bucket structure with hydrophobic 'rim') which can support TPeAB in producing clouding phenomenon. However, glycine is a typical hydrophilic molecule which may withdraw surface water and responsible for dehydration of micelle with a concomitant CP decrease. A similar type of CP decrease in presence of alkanols has been interpreted by taking hydrophobic interactions into consideration [37]. It may be mentioned here that glycine is distinctly less effective in decreasing the CP of the chosen system and, therefore, rule out for the solubilization study.

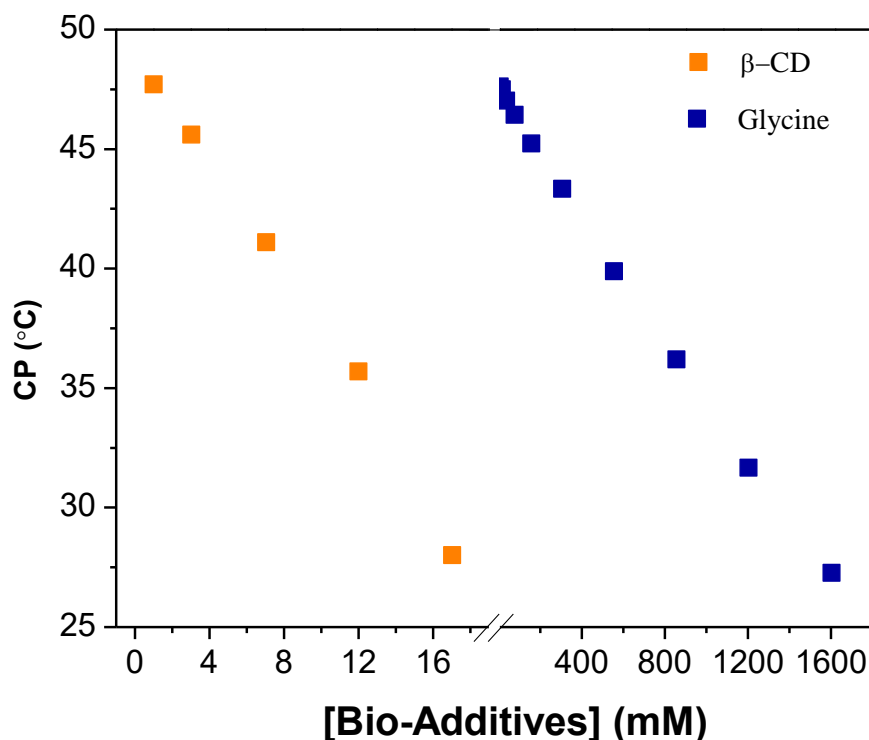


Figure 11. Variation of CP with β -CD and glycine

4.4. PAH Solubilization Studies in TPeAB+ 12-4-12A with and without β -CD

4.4.1. Interplay of [12-4-12A], [TPeAB] and CP on Single PAH Solubilization

Based on CP variation (Figure 8), sample (having CP at 40°C) has been chosen for anthracene solubilization (Table 5) and to compare it at 30°C (for the same system). Anthracene has been selected for solubilization as it has least aqueous solubility (among all the PAHs studied here) in aqueous, micellar and mixed micellar systems [38, 39]. The idea behind this experiment (Table 5) was to exploit the advantages of SAIL mixed system together with *clouding phenomenon* (and also temperature effect). It has been reported that hydrophobicity of the surfactant system has been found maximum just below the CP [33].

Anthracene solubilization (MSR value, computing procedure given in **Chapter 2, 2.5.11**) in individual aqueous TPeAB (80 mM) has been found less than individual aqueous 12-4-12A (at cmc), at two different temperatures. However, mixing of the above two components (80 mM TPeAB + 1 mM 12-4-12A) causes an increase in anthracene solubilization. MSR increases further as this system approaches the CP (40°C). MSR, under the similar conditions (40°C and 80 mM TPeAB), increases with [12-4-12A] to 2 mM. However, a further increase of [12-4-12A] or [TPeAB] causes a decrease in anthracene MSR. This allows us to choose 2 mM 12-4-12A + 80 mM TPeAB system for the solubilization study of other PAHs (pyrene and fluorene) at both temperatures (30°C and at just below CP (40°C)). Again, pyrene and fluorene solubilization increases near CP as observed with anthracene. Therefore, CP has a distinct influence on solubilization phenomenon of PAHs which may be due to structural growth near CP [28, 33].

4.4.2. Solubilization of PAHs in 12-4-12A + TPeAB + β -cyclodextrin System

Recently, extraction of PAHs from soil has been reported in aqueous β -cyclodextrin (β -CD)[40]. Table 5 also shows MSR data related to solubilization of PAHs in the system, having CP 40°C, adjusted by β -CD (which reduces the requirement of TPeAB to 38mM). The system is greener (due to β -CD) and also showed better solubilization potential, for anthracene than the system containing 80 mM TPeAB, (Table 5). However, the system shows a limitation towards pyrene solubilization. This may be due to different solubilization sites of anthracene and pyrene in the micellar system. Anthracene solubilizes in the outer region of the micellar interior while pyrene goes in the inner micellar core [41]. β -CD has several hydroxyl groups together with the hydrophobic region in the rim of the bucket type structure. Probably, due to the above

structural features, the β -CD system is more effective towards anthracene solubilization. To get insight into the morphologies present in the above two systems (with and without β -CD), TEM micrographs were acquired (Figure 12). A system with β -CD shows more compact structures as compared to open fragmented/ smaller structures seen in the sample without β -CD with 80 mM or 38 mM TPeAB. Probably these compact structures are responsible for higher MSR with anthracene. Moreover, such a system may also find potential application for extracting thermo-responsive biological compounds such as vitamins, proteins, drugs, nucleotides etc [42, 43]. However, the cost of β -CD may increase the overall cost of the process and should be preferred only for the solubilization of precious biomolecules.

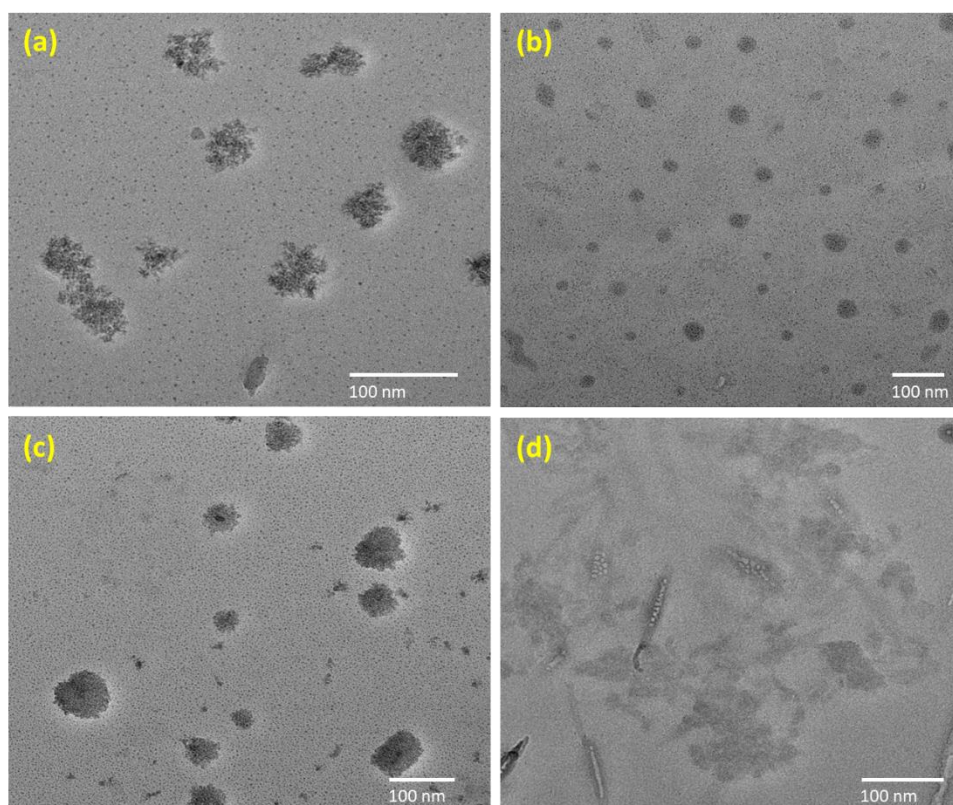


Figure 12. Negative stained TEM images of aggregates of 2 mM 12-4-12-A with: (a) 80 mM TPeAB, (b) 38mM TPeAB; (c) 38 mM TPeAB + 7.3 mM β -CD (d) 38mM TPeAB; (c) 38 mM TPeAB + 700 mM glycine.

Table 5. Molar Solubilization Ratio (MSR) of PAHs in different aqueous single and mixed (12-4-12A + TPeAB) system at room temperature (30°C) and near cloud point (39°C).

Systems	MSR					
	30 °C	39 °C (~ CP)	30 °C	39 °C (~ CP)	30 °C	39 °C (~ CP)
TPeAB (80mM)	0.000042	0.000063	-	-	-	-
12-4-12A	0.0012	0.0024	0.0061	-	0.0205	-
12-4-12A (10mM)	0.0261	0.0293	0.0381	-	0.0910	-
12-4-12A(1mM) + TPeAB (80mM)	0.0103	0.0115	-	-	-	-
12-4-12A (2mM) + TPeAB (80mM)	0.0119	0.0143	0.113	0.122	0.165	0.210
12-4-12A (5mM) + TPeAB (80mM)	0.0058	0.0066	-	-	-	-
12-4-12A(10mM) + TPeAB (86mM)	0.0032	0.0046	-	-	-	-
12-4-12A (2mM) + TPeAB(38mM) + β-Cyclodextrin(7.3mM)	0.0226	0.0264	0.0817	0.0896	-	-

4.5. Co-solubilization of PAHs

Since PAH contaminated sites (*e.g.*, aquatic and soil matrix) contains a mixture of different PAHs, multiples PAHs solubilization can mimic the situation for selective micellar solubilization from different PAHs. For the purpose, co-solubilization of three different pairs of PAHs selected and solubilization studies are performed in 2 mM 12-4-12A+ 80 mM TPeAB. The co-solubilization data are compiled in Table 6. Data show that solubilization of an individual PAH can increase or decrease on co-solubilization of another PAH(s). As mentioned earlier, the solubilization site of a particular PAH has a role to play in the co-solubilization of more than one PAH. If the solubilization site is common for the PAHs in the pair, the solubilization content of one of them may decrease. However, if the two PAHs has different micellar solubilization sites, their mutual presence may increase solubilization content due to increased hydrophobic interactions caused by the presence of PAHs. This indeed was observed in Table 6. Here, MSR values of anthracene increases in the presence of pyrene and nearly remain constant in fluorene. However, fluorene MSR decreases in the presence of anthracene than without anthracene. Additionally, pyrene solubilization (singly or with other PAHs) shows a remarkable increase in the presence of other PAHs. The increase was higher in case of fluorene than the anthracene. This may be due to higher MSR of fluorene in comparison of anthracene (single solubilization) which subsequently provide more hydrophobicity to the micelle and concomitant higher solubilization of pyrene. This indeed observed from our co-solubilization experiment (Table 6, and Figure 13)

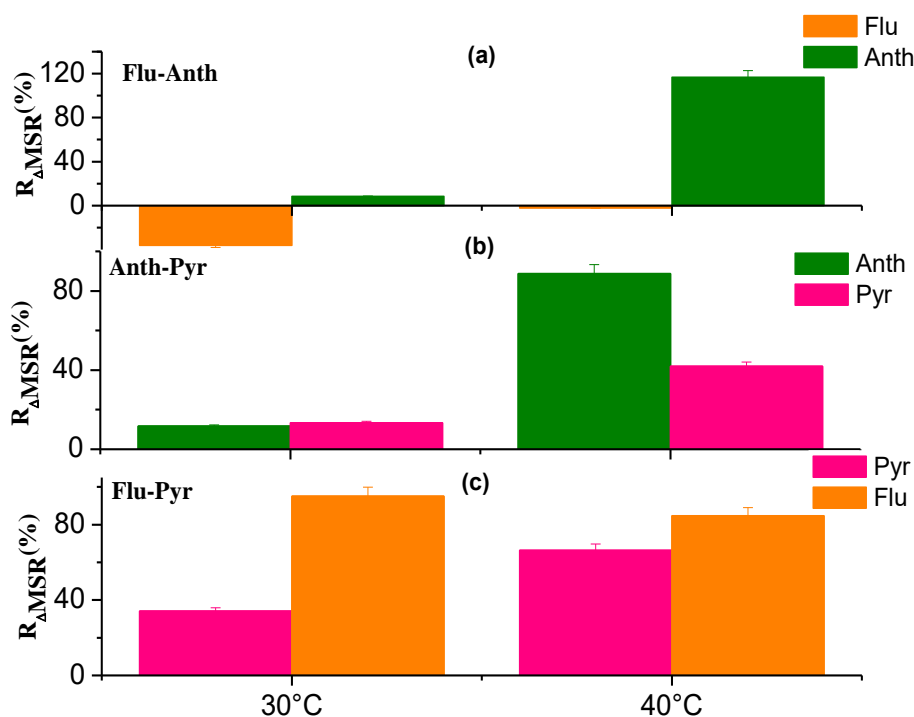


Figure 13. Change in solubilization ($R_{\Delta MSR}$) % of individual PAH (in pair) at 30°C and 40°C (just below the CP) in 2 mM 12-4-12A+ 80 mM TPeAB system: (a) Anthracene (Anth) - Fluorene (Flu); (b) Anthracene (Anth) – Pyrene (Pyr); (c) Pyrene (Pyr) - Fluorene (Flu).

4.6. Extraction/ Adsorption of PAH

Anthracene solubilized systems with or without β -CD are used for the extraction process. Anthracene has been found to partition in SRP preferentially (Figure 14) over surfactant lean phase (SLP). Almost all anthracene has been concentrated in SRP of the system without β -CD. The lower content of anthracene, in the β -CD containing system, may be due to the partitioning of β -CD both in SRP and SLP. β -CD in SLP can solubilize more anthracene and restrict it to go in SRP. This proposition may find support from the fact that β -CD contain several -OH groups which have a certain preference for water and making it β -CD + water mixed solvent (probably less polar) and prefer to bind with anthracene as reported in a recent study [40]. SRP with extracted

anthracene has been used to determine the adsorption potential of GZrO₂ nanocomposite. Figure 14 shows that no anthracene left in the diluted SRP solution indicating nearly complete adsorption on the composite. The information can be used for the possible degradation of anthracene from the adsorbed state. This may find support from a recent report in which graphene-Titanium oxide has been used to photodegrade polyaromatic hydrocarbon [44]. It is expected that the nanocomposite (Gr@ZrO₂-NC) exhibits augmented hybrid properties (from both the constituent) and have potential applications in the field of catalysis/ photocatalysis [45].

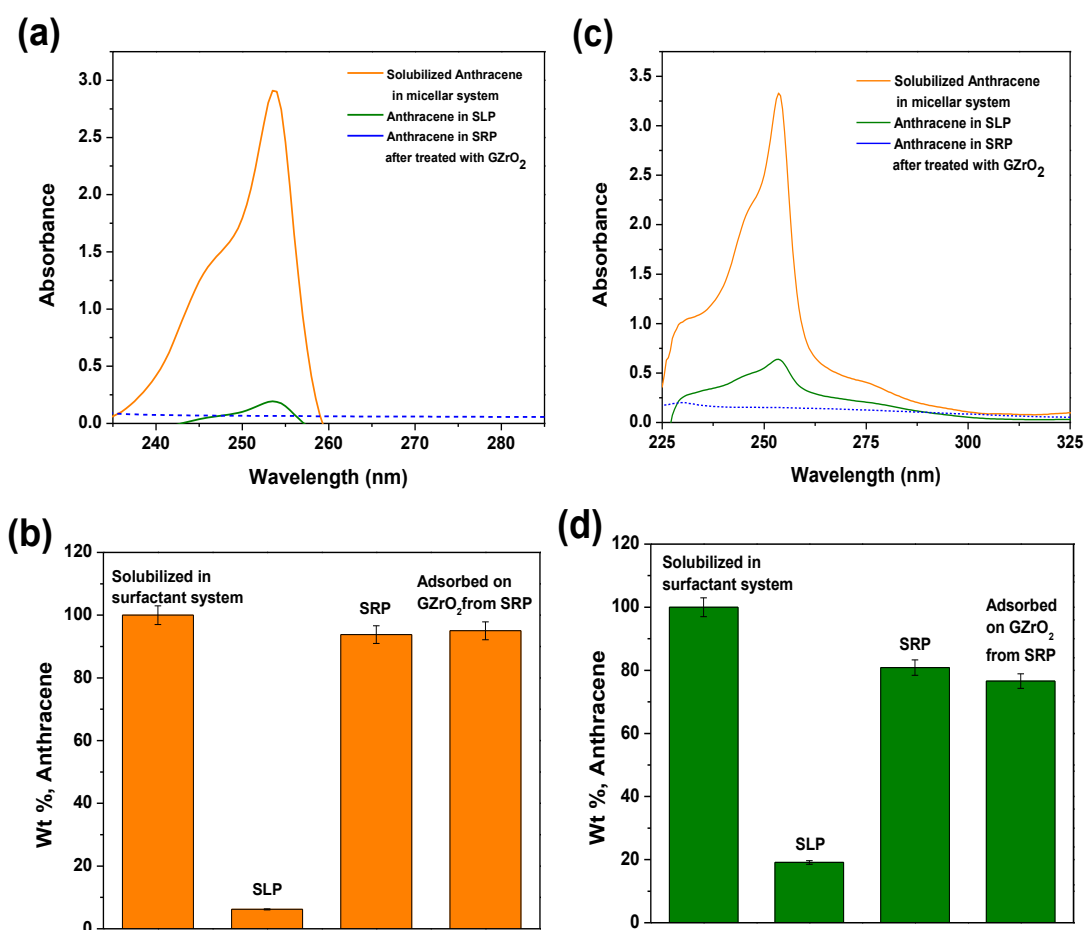
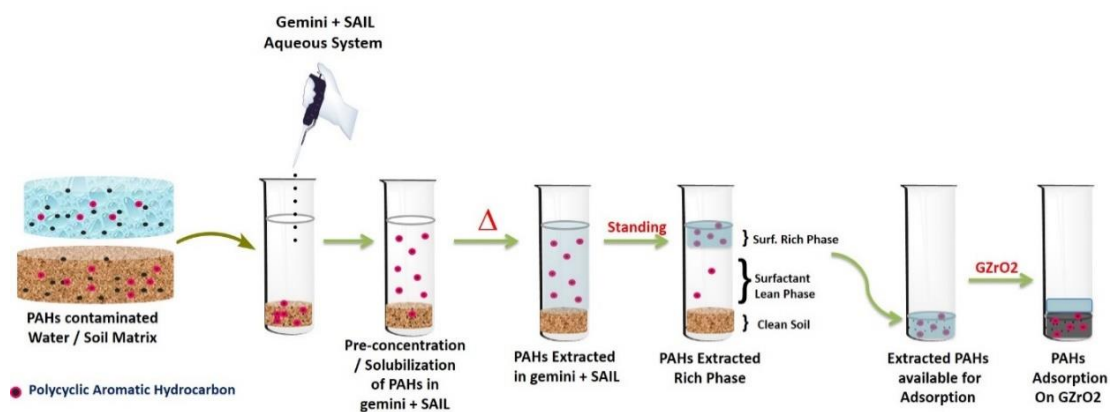


Figure 14. UV spectra of Anthracene solubilization in : (a, b) 2mM 12-4-12 A + 80 mM TPeAB and (c, d) 2mM 12-4-12 A + 38 mM TPeAB + 7.3 mM β- CD; before (—), after phase separation in surfactant lean phase (—) and after adsorption on GZrO₂ nanocomposite from surfactant-rich phase (.....).

Table 6. PAHs solubilization parameters (molar solubilisation ratio, MSR; micelle-aqueous phase partition coefficient, $\ln K_m$) of 2 mM 12-4-12A + 80 mM TPeAB in aqueous solution at two different temperatures (T).

T (°C)	Anth	Anth-Pyr	Anth-Flu	Pyr	Pyr-Anth	Pyr-Flu	Flu	Flu-Anth	Flu-Pyr
MSR									
30.0	0.012	0.013	0.013	0.113	0.129	0.152	0.165	0.105	0.322
39.5	0.014	0.027	0.031	0.122	0.173	0.203	0.210	0.205	0.388
$\ln K_m$									
30.0	8.08	8.07	8.17	10.4	10.14	10.12	10.88	10.49	10.37
39.5	8.27	8.24	9.18	10.3	10.16	10.15	11.13	10.62	10.50



Scheme 1. Representation of extraction and degradation of PAHs.

4.7. Conclusion

This study was planned to exploit the positivity of the surfactant research such as (1) performance of gemini (anionic) over conventional surfactant, (2) synergism of mixed systems over individual ones, (3) CP observance with 12-4-12A (with a SAIL, TPeAB) (4) tuning of CP with biocompatible material (amino acid or cyclodextrin) (5) CP observance at ambient temperature ($\sim 40^{\circ}\text{C}$) with lower [12-4-12 A] (2mM) and [TPeAB] (38 mM, in presence of 7mM β -CD) and (6) solubilization of PAHs at different temperatures. Interaction and morphologies of the aggregates are confirmed by ^1H NMR and POM / TEM studies. POM data show bigger aggregates near CP while TEM results show the formation of compact aggregates in the presence of β -CD. By adopting the above strategies, it was possible to increase MSR for anthracene (least soluble PAH of the present study) from 0.012 to 0.031 (2.58 times). A similar increase was found with other PAHs. However, solubilization enhancement depends upon nature and site of solubilization of a particular PAH (singly or in the mixture). The study may find potential applications in increasing the bioavailability of the hydrophobic material (PAHs, drugs, pesticides, organic pollutant etc.) and their subsequent biodegradation (Scheme 1) [46]. The finding of the study can be useful in remediation of soil. The work in this direction is already going on in our laboratory.

References

- [1] K. Dong, X. Liu, H. Dong, X. Zhang, and S. Zhang, *Chem. Rev.* 2017, 117, 6636-6695.
- [2] J.P. Hallett and T. Welton, *Chem. Rev.* 2011, 111, 3508-3576.
- [3] C.J. Margulis, *Mol. Phys.* 2004, 102, 829-838.
- [4] H. Wang, L. Zhang, J. Wang, Z. Li and S. Zhang, *Chem. Comm.*, 2013, 49, 5222-5224.
- [5] X. Liu, G. Zhou, F. Huo, J. Wang and S. Zhang, *J. Phys. Chem. C.* 2015, 120, 659-667.
- [6] B. Dong, N. Li, L. Zheng, L. Yu, and T. Inoue. *Langmuir*, 2007, 23, 4178-4182.
- [7] N. Cheng, P. Yu, T. Wang, X. Sheng, Y. Bi, Y. Gong and L. Yu, *J. Phys. Chem. B*, 2014, 118, 2758-2768.
- [8] A. Triolo, O. Russina, B. Fazio, G.B. Appetecchi, M. Carewska and S. Passerini, *J. Chem. Phys.* 2009, 130, 164521.
- [9] J. Wang, H. Wang, S. Zhang, H. Zhang and Y. Zhao, *J. Phys. Chem. B.* 2007, 111, 6181-6188.
- [10] H. Wang, Q. Feng, J. Wang and H. Zhang, *J. Phys. Chem. B.* 2010, 114, 1380-1387.
- [11] Y. Zhao, S. Gao, J. Wang and J. Tang, *J. Phys. Chem. B.* 2008, 112, 2031-2039.
- [12] L. Leclercq and A.R. Schmitzer, *J. Phys. Chem. A.* 2008, 112, 4996-5001.
- [13] S. Palchowdhury and B.L. Bhargava. *J. Phys. Chem. B.* 2014, 118, 6241-6249.
- [14] S. Kumar, D. Sharma and Kabir-ud-Din*. *Langmuir.* 2003, 19, 3539-3541.
- [15] S. Kumar and Z.A. Khan, *J. surfactants. Deterg.* 2004, 7, 367-371.
- [16] B.L. Bales and R. Zana, *Langmuir.* 2004, 20, 1579-1581.
- [17] G.C. Kalur and S.R. Raghavan, *J. Phys. Chem B.* 2005, 109, 8599-8604.
- [18] D.T. Kamei, D.I. Wang and D. Blankschtein, *Langmuir.* 2002, 18, 3047-3057.
- [19] F.A. Vicente, L.P. Malpiedi, F.A. e Silva, Jr, A. Pessoa, J.A. Coutinho and S.P. Ventura, *Sep. Purif. Technol.* 2014, 135, 259-267
- [20] D. Xie and J. Zhao, *RSC Adv.* 2016, 6, 27031-27038.

- [21] F.A. Vicente, I.S. Cardoso, T.E. Sintra, J. Lemus, E.F. Marques, S.P. Ventura and J.A. Coutinho, *J. Phys. Chem. B.* 2017, 121, 8742-8755.
- [22] P. M. Holland and D. N. Rubingh, *J. Phys. Chem.* 1983, 87, 1984-1990.
- [23] M. A. Sanchez-Trujillo, E. Morillo, J. Villaverde and S. Lacorte, *Environ. Pollut.* 2013, 178, 52-58.
- [24] J. H. Clint, *J. Chem. Soc. Faraday Trans 1: Physical Chemistry in Condensed Phases* 1975, 71, 1327-1334
- [25] D. N. Rubingh, K. L. Mittal, *Solution Chemistry of Surfactants*, Plenum Press: New York, 1979; Vol. 1, p337.
- [26] K. Motomura, M. Yamanaka and M. Aratono, *Colloid Polym. Sci.* 1984, 262, 948-955.
- [27] L. Liu and M. J. Rosen, *J. Colloid Interface Sci.* 1996, 179, 454-459.
- [28] A. Bhadoria, S. Kumar, V. K. Aswal and S. Kumar, *RSC Adv.* 2015, 5, 23778-23786.
- [29] P. Mukherjee, K.S. Pradhan, S. Dash, S. Patel, and B.K. Mishra, *Adv. colloid interface sci.* 2011,162, 59-79.
- [30] L. B. Bales and R. Zana, *Langmuir.* 2004, 20, 1579-1581.
- [31] A. Mats and S. Swarup, *J. Phy. Chem.* 1983,87, 876-881.
- [32] U. Thapa, J. Dey. S. Kumar, P.A. Hassan, V.K. Aswal and K. Ismail, *Soft Matter.* 2013, 9, 11225-11232
- [33] S. Kumar, A. Bhadoria, H. Patel and V. K. Aswal, *J. Phy. Chem. B.* 2012,116, 3699-3703.
- [34] Kabir-ud-din, D. Sharma, Z. A. Khan, V. K. Aswal and S. Kumar, *J. Colloid Interface Sci.* 2006, 302, 315-321.
- [35] E. Junquera, G. Tardajos and E. Aicart, *Langmuir.* 1993, 9, 1213-1219.
- [36] R. Palepu and J.E. Richardson, *Langmuir.* 1989, 5, 218-221.
- [37] T. Ahmad, S. Kumar, Z. A. Khan and Kabir-ud-Din, *Colloids Surf A.* 2007, 294, 130-136.
- [38] J. Lakra, D. Tikariha, T. Yadav, S. Das, S. Ghosh, M. L. Satnami, and K. K. Ghosh, *Colloids Surf A.* 2014, 451, 56-65.
- [39] S. K. Yadav, K. Parikh and S. Kumar, *Colloids Surf. A.* 2017, 514, 47-55
- [40] M. A. Sanchez-Trujillo, E. Morillo, J. Villaverde and S. Lacorte, *Environ. Pollut.* 2013, 178, 52-58.

- [41] N. Fatma, M. Panda, W. H. Ansari and Kabir-ud-din, *Colloids Surf. A*. 2015, 467, 9-17.
- [42] S. Kumar, M. S. Alam, N. Parveen, and Kabir-ud-din, *Colloid Polym Sci*. 2006, 284, 1459-1463.
- [43] A. S. Yazdi, *Trends Anal Chem*. 2011, 30, 918-929.
- [44] H. Bai, J. Zhou, H. Zhang, and G. Tang, *Colloids Surf B: Biointerfaces*. 2017, 150, 68-77.
- [45] B.R. Singh, M. Shoeb, W. Khan and A. H. Naqvi, *J. Alloys Compd*. 2015, 651, 598-607
- [46] A. Rodrigues, R. Nogueira, L. F. Melo, and A. G. Brito, *Int Biodeterior. Biodegradation*. 2013, 83, 48-55.